ACADEMIA ROMÂNĂ
Revue Roumaine de Chimie
http://web.icf.ro/rrch/

Rev. Roum. Chim.,
2021, *66*(10-11), 855–869
DOI: 10.33224/rrch.2021.66.10-11.09

Dedicated to the memory of
Prof. Petre T. FRANGOPOL (1933-2020)

INTERACTION OF LOCAL ANESTHETIC PROCAINE WITH PHOSPHOLIPID MODEL MEMBRANE

Aurora MOCANU,[a] Peter J. QUINN,[b] Cristina NICULA,[c] Sorin RIGA,[a,d] Gheorghe TOMOAIA,[d,e] Ciprian-Alin BARDAŞ[e] and Maria TOMOAIA-COTISEL[a,d,*]

[a]Babeş-Bolyai University, Faculty of Chemistry and Chemical Engineering, Department of Chemical Engineering, Research Center of Physical Chemistry, 11 Arany Janos Street, 400028, Cluj-Napoca, Roumania
[b]King's College London, Department of Biochemistry and Biophysics, Campden Hill Road, London W8 7AH, United Kingdom
[c]Iuliu Haţieganu University of Medicine and Pharmacy, Ophthalmology, 8 Victor Babeş Street, 400012, Cluj-Napoca, Roumania
[d]Academy of Romanian Scientists, 3 Ilfov Street, Sector 5, RO-050044, Bucureşti, Roumania
[e]Iuliu Haţieganu University of Medicine and Pharmacy, Department of Orthopedics and Traumatology, 47 General Traian Mosoiu Street, 400132, Cluj-Napoca, Roumania

Received November 2, 2021

The interaction of local anesthetic procaine, PR, with dipalmitoyl phosphatidylcholine (DPPC) model membranes was investigated at the air-water interface using Langmuir technique (LT), Langmuir-Blodgett self-assemblies technique (LBT) and atomic force microscopy (AFM). Compressional isotherms were interpreted by surface solution thermodynamic approach and AFM images on the LB layers transferred on mica substrate, at various surface pressures. Results have demonstrated the procaine penetration into the DPPC monolayer membrane and showed changes in the membrane structure with the increasing of both the procaine concentration and the lateral surface pressure. PR molecules penetrate within DPPC membrane and have a strong effect on the membrane structure, facilitating the membrane fluidity while maintaining a great stability of phospholipid membrane at the highest surface pressures, at DPPC monolayer membrane collapse. Finally, it is postulated that the pressure dependence of the penetration of procaine into phospholipid model membranes might be of relevance in the interfacial mechanism of pressure reversal in anesthesia.

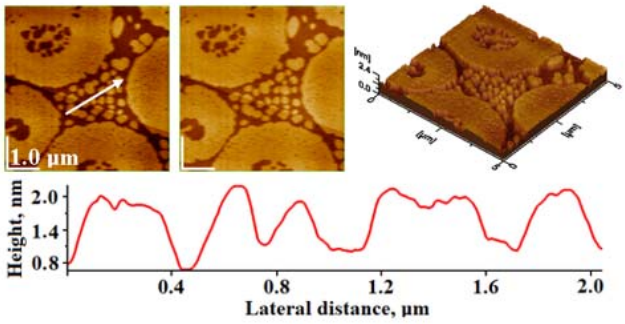

INTRODUCTION

Local anesthetics are drugs that have the ability to form intermolecular hydrogen bonds with water, lipid, and protein molecules that might control the membrane structure and block the nervous impulse causing a local loss of sensation including pain in a specific part of the body. Although there are several theories to describe their mode of action, still there is an ongoing debate.[1-3]

Molecular mechanisms by which anesthetic action takes place on nerve membranes effectively fall at least into two main categories. Anesthetics may act indirectly on proteins via perturbations of their surrounding lipids, or directly by closing the sodium channels, thus blocking nerve signal

* Corresponding author: mcotisel@gmail.com

propagation. Since it is not always clear which type of action occurs, both mechanisms must be considered.

Studies of anesthetic action have been performed using both intact nerve systems[1] and various model membrane systems.[4-43] The findings show that anesthetics are bound to the lipid membrane, increasing the fluidity of the lipid portion of the membrane by decreasing the order of the hydrocarbon chains. Although these studies involved different physical parameters, the molecular origin of the observed effects are presumably the same, viz. the modification of the structural properties of ordered acyl chains due to the binding of anesthetics into oriented lipid systems.

The quantitative treatment of the interaction of anesthetics with lipid membrane model systems such as monolayers or bilayers is a fundamental problem in biophysics. Monolayer membrane models may be justified as representing one half of a bilayer[19,20] and providing useful information, at the molecular level, on the conformation and packing of the membrane components under conditions similar to those encountered in vivo.[19-21] In addition, such membrane films permit the quantitative examination of interactions between the film-forming molecules and subphase components such as anesthetics, by using a thermodynamic approach.

A few studies were carried out using procaine related tertiary amine anesthetics. Procaine is an ester of 4-aminobenzoic acid with 2-diethyl aminoethanol, *i.e.*, $4\text{-}H_2NC_6H_4CO_2[CH_2CH_2N(C_2H_5)_2]$, PR.[16-18,22,23] Studies suggest that procaine and procaine analogous intercalate into the lipid systems. Moreover, work of our group[16-18,38-41] has shown that the location of procaine and its effects on the monolayer properties of the lipids to be dependent on the charge of the procaine molecule and on the surface characteristics of the chosen lipid.

The phase behavior of lipids, fatty acids and proteins in a monolayer model in the absence and the presence of drugs, such as anesthetics, has been the subject of various investigations, by Langmuir-Blodgett, LB, monolayer film technique, which is an effective tool to transfer self-assembled biomolecules from a fluid interface to a solid substrate and further visualized by atomic force microscopy, AFM. The advantage of the LB technique is to prepare the controlled molecular architecture obtained on aqueous subphase by adjusting certain parameters, like pH, ionic strength, molar composition, temperature and surface lateral pressure.

Our results have shown elsewhere that alternative contact, AC tapping mode AFM provides good imaging of organic molecules in self-assembled monolayers on various solid surfaces, like glass and mica substrate[44-53] in substantial agreement with AFM studies on related membrane models.[54-64]

In this study we extend these experiments to examine the interaction of protonated procaine [procaine hydrochloride: $PR{\cdot}H^+Cl^-$] with L-α-dipalmitoyl phosphatidylcholine (DPPC) monolayer membrane at the air/aqueous solution interface. For the first time, the penetration of cationic procaine, $PR{\cdot}H^+$ noted also simple PR, into DPPC monolayer membrane is explore by thermodynamic approach and is correlated with morphology of DPPC membrane visualized with AFM, in tapping mode, offering complementary images (*e.g.*, 2D-topography, phase image, amplitude image and 3D-topography), surface roughness and the size and shapes of various phospholipid domains.

In this work, we show our advances in tapping AFM imaging with superior lateral and z (height) resolution (about 0.1 nm) of DPPC membrane in the absence and the presence of local anesthetic procaine, PR. Also, a main focus in this study involves the well-designed experiments, like DPPC and DPPC-PR membrane transferred on mica surface by LBT at suitable PR concentrations (*e.g.*, 10^{-4} M and 10^{-3} M) at various lateral surface pressures, including the phase transition where the coexistence of liquid expanded, LE, and liquid condensed, LC, can be visualized.

It is worth mentioning that our group also used AFM for exploration of inorganic nanoparticles and hybrid (organic-inorganic) materials[65-69] leading to the development of better quality nanomaterials[70-73] designed for tissue engineering.

RESULTS AND DISCUSSION

Compressional isotherms of DPPC model membranes: Thermodynamic approach

In order to investigate the penetration of protonated procaine (PHR^+, component 2), dissolved in water (component 1), into dipalmitoyl phosphatidylcholine (DPPC, component 3) monolayer membranes, the π versus A_3 compression isotherm were recorded for DPPC films spread on unbuffered aqueous subphases containing procaine hydrochloride at various concentrations (c_2) between 0 and 10^{-2} M. A_3 represents the mean molecular area of DPPC obtained by dividing the area of the lipid monolayer to the number of lipid molecules spread at the interface.

Compressional isotherm of DPPC monolayers in the absence and presence of protonated procaine are presented in Figs. 1A and 1B.

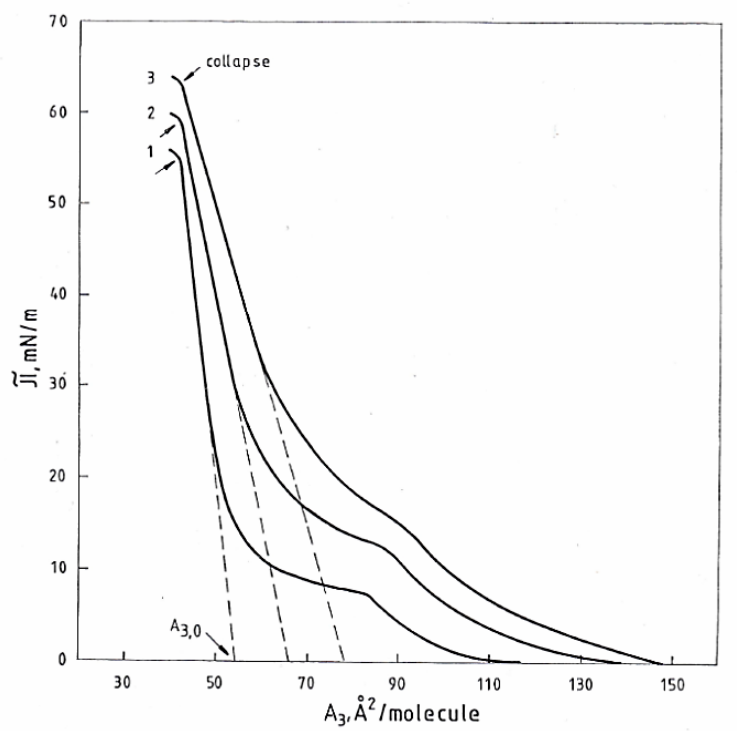

Fig. 1A – Compressional isotherms in terms of surface pressure (π) *versus* mean molecular area (A_3) of DPPC in monolayer membranes spread at the air-aqueous PR·HCl solution interface for c_2: curve (1) 0; (2) 10^{-5} M; (3) 10^{-3} M; $A_{3,0}$ represents the limiting molecular area of DPPC.

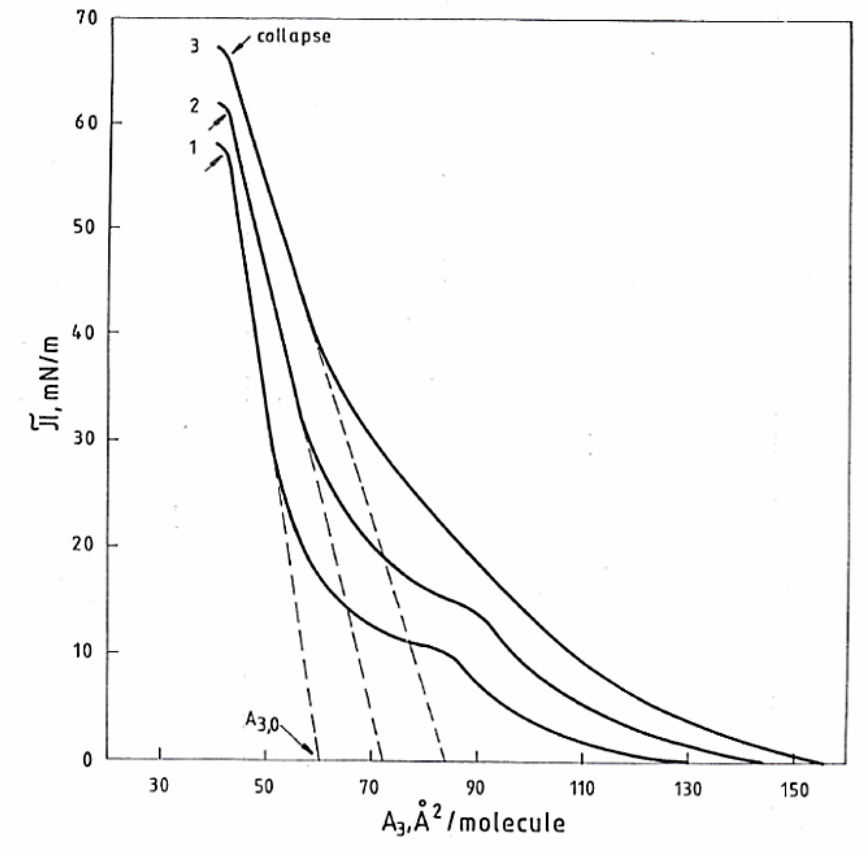

Fig. 1B – Compression isotherms of π *versus* A_3 of DPPC membranes spread at the air-aqueous PR·HCl solution interface for c_2: curve (1) 10^{-6}; (2) 10^{-4}; (3) 10^{-2} M; symbols as in Fig. 1A.

Table 1

Monolayer characteristics of DPPC membrane spread on various PRH^+ concentrations in aqueous subphase

c_2, M	0	10^{-6}	10^{-5}	10^{-4}	10^{-3}	10^{-2}
$A_{3,0}$ (nm^2/molecule)	0.54	0.60	0.66	0.71	0.77	0.84
$A_{3,c}$ (nm^2/molecule)	0.42	0.42	0.42	0.42	0.42	0.42
π_c, mN/m	54	57	58	60	63	66
$C_{s,0}^{-1}$, mN/m	225	190	159	147	138	132

From these curves it is noticeable that the most important effect of the subphase PRH^+ upon the compressional isotherms is to expand the phospholipid monolayer membrane while reducing and eventually eliminating the LE/LC phase transition, being so persistent in the absence of subphase drug.[18,31,42] In the case of pure DPPC membrane the LE/LC phase transition occurs at a surface pressure of 8 mN/m, as observed on curve 1, in Fig. 1A. Further, one may observe that at constant pressure the mean molecular area increases with increasing PRH^+ concentration c_2 in the subphase making the films more compressible. Also, Figs. 1A and 1B show that the collapse pressure, π_c, increases with increasing c_2, reflecting the stabilizing effect of the subphase PRH^+ on condensed phospholipid monolayer membrane.

Based on molecular model calculations of the area requirements of the polar head group of DPPC, we put forward the hypothesis that this LE/LC phase transition involves a conformational transition between the "zwitterion" and the "internal salt" conformations[31] of the polar head group. This presumption seems to be in agreement with literature data.[18, 28-31] As can be seen from Fig. 1A, curve 2 at c_2 equals 10^{-5} M, the phase transition occurs with the horizontal portion virtually reduced, while at the highest PRH^+ concentration of 10^{-2} M it vanishes completely (curve 3, in Fig. 1B).

From the compressional isotherms (Figs 1A and 1B) the following surface characteristics for DPPC monolayer membranes in the absence and in the presence of protonated procaine have been derived: ($A_{3,0}$) - the limiting molecular area is obtained by extrapolation to $\pi = 0$ of the condensed linear portion of the isotherm, as shown by dashed straight lines; ($A_{3,c}$) - the collapse area is the molecular area corresponding to the sudden slope change of the isotherm at the highest π values (still in monolayer state) named the collapse pressures (π_c), as indicated by arrows; and the limiting surface compressional modulus, $C_{s,0}^{-1}$, defined as:

$$C_{s,0}^{-1} = -A_{3,0}\left(\frac{\partial \pi}{\partial A_3}\right)_T = -A_{3,0}\frac{\pi_c}{A_{3,c} - A_{3,0}}$$

The magnitudes of the quantities defined above, as obtained from the experimental data illustrated in Figs. 1A and 1B, are presented in Table 1.

The expansion effects are obvious from the significant increase of $A_{3,0}$ with increasing c_2. The fluidizing effect is shown by the decrease of $C_{s,0}^{-1}$ with increasing c_2. Both effects support the proposed penetration of PRH^+ molecules from the subphase into the DPPC monolayer membrane. On the other hand, both Figs. 1A and 1B as well as Table 1 show that the collapse area of DPPC is unaffected by the subphase PRH^+. Irrespective of c_2, the $A_{3,c}$ has the same value, suggesting that at the highest surface pressures the PRH^+ molecules are squeezed out from the DPPC monolayer membrane.

In spite of the expulsion of PRH^+ molecules near the DPPC membrane collapse, π_c increases with increasing c_2 in the subphase, i.e. PRH^+ ions stabilize the condensed DPPC monolayer membrane. Presumably, the expelled PRH^+ molecules do not diffuse into the bulk subphase, but form a Gibbs - type PRH^+ monolayer, beneath the insoluble DPPC monolayer membrane and a specific interaction occurs between them, stabilizing the DPPC model membrane.

From a quantitative point of view, PRH^+ penetration into the DPPC monolayer can be studied by means of Gibb's equation, which in the presence of a DPPC monolayer, may be written[17,33-36] as:

$$\Gamma_2' = \frac{1}{kT}\left(\frac{\partial \pi}{\partial \ln c_2}\right)_{A_{3,T}} \quad (1)$$

where Γ_2' stands for the amount of adsorption of the PRH^+ per unit area of free interface, (i.e. not covered by DPPC); c_2 represents the molar concentration of PRH^+ in the aqueous subphase; k and T are the Boltzmann constant and the absolute temperature, respectively.

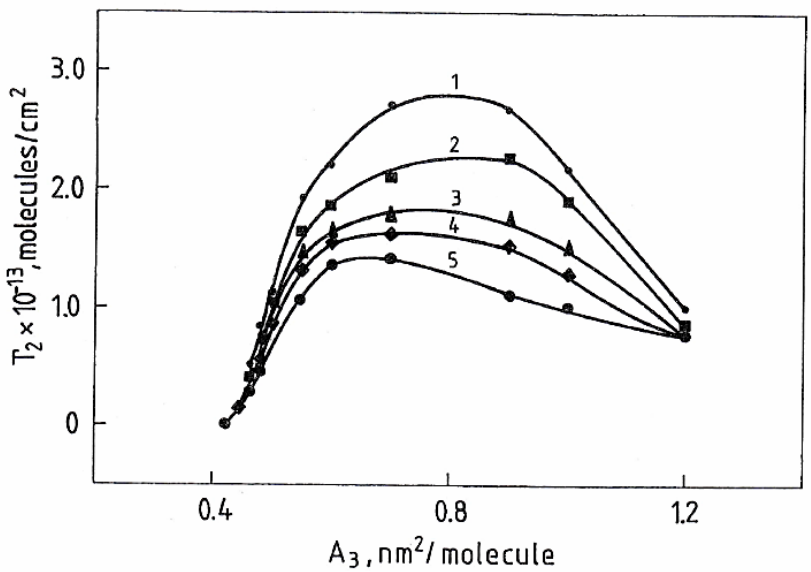

Fig. 3B – Adsorption of PRH^+ species (Γ_2, molecules/cm^2) per unit of the interface at various c_2 values; symbols as in Fig. 3A.

The extent to which PRH^+ penetrates the DPPC monolayer spread at an air/water interface can be characterized by means of the penetration number (n_p) defined as the ratio of the number of PRH^+ ions to DPPC molecules at the interface, *i.e.*:

$$n_p = \frac{N_2}{N_3} \tag{4}$$

By taking into account Eq. (2) and by using the approach $\overline{A}_3 = A_{3,c}$, one obtains

$$n_p = A_3\Gamma_2 = (A_3 - A_{3,c})\Gamma_2' \tag{5}$$

Penetration numbers calculated by means of Eq. (5) are plotted vs. A_3 in Fig. 4.

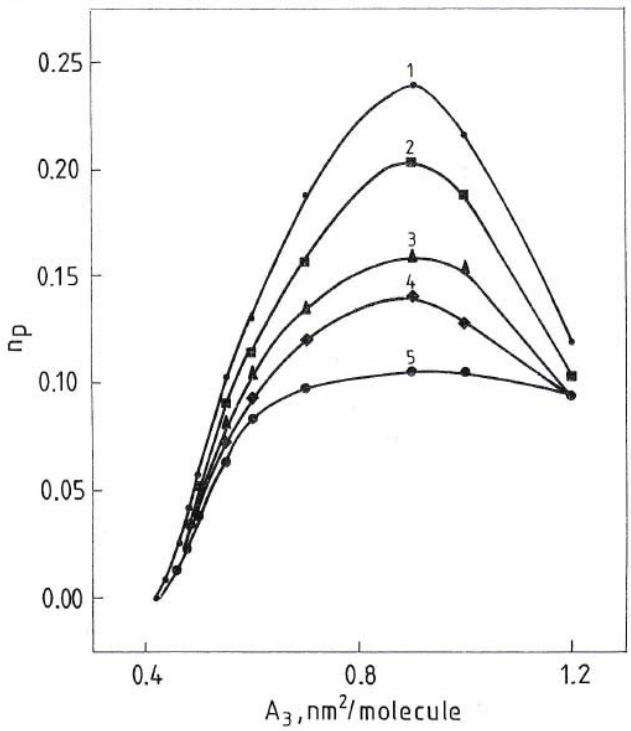

Fig. 4 – Penetration numbers (n_p) as a function of A_3 values for DPPC monolayer membranes spread on various PRH^+ concentrations; symbols as in Figs. 3A and 3B.

The maximum n_p values are observed in the same A_3 region, irrespective of the value of c_2. In contrast, the surface pressure corresponding to the maximum n_p value is very much affected by c_2, vis. π increases with increasing c_2. For example, one has the maximum n_p at $c_2 = 10^{-6}$ M for $\pi \approx 10$ mN/m, whereas at $c_2 = 10^{-2}$ M it attains $\pi \approx 20$ mN/m.

It is interesting to compare values of the maximum penetration number with those obtained earlier for the penetration of PRH^+ in SA monolayers under identical conditions, vis. with SA spread on unbuffered aqueous solutions of protonated procaine.[13] It seems that PRH^+ penetrates much more easily into DPPC monolayers than into the SA ones. Presumably, this is due in part to the less compact character of the DPPC monolayers, when compared to those of SA under similar conditions.

On the other hand, the PRH^+/DPPC binding energy presumably arises from hydrophobic and polar interactions, resulting in the stabilization of the procaine dipole (ester bond) in the lipid dipole region at the air/water interface and from interactions of the protonated tertiary amine of procaine, either with the polar head groups of the lipids, or directly with the zwitterion lattice. It is expected the procaine molecules to shuttle relatively rapidly between deeper and shallower sites (toward the polar head group of lipid) depending on the charge of procaine molecule.

The effect of the insoluble lipid monolayer to enhance the PR adsorption is due mainly to the hydrophobic interactions between the molecules of both surfactants, but it is strongly influenced also by the compactness of the DPPC monolayer membrane.

The hydrophobic moiety of the PR molecule is of small dimensions and, consequently, in its interaction with the long hydrocarbon chains of the insoluble surfactants no important differences may arise. Thus, the different behavior might be assigned to the hydrophobic interactions between the molecules of the insoluble surfactant themselves. The attracting forces between the neighboring molecules will be the most important in the case of SA, having a small polar group and a single saturated hydrocarbon chain and SA will give the most compact film, being the most disadvantageous for the PR penetration.

Penetration number values obtained in this study are comparable to those calculated for norleucine from literature data obtained with dimyristoyl phosphatidylcholine monolayers.[34] However, these values are much lower than those reported for the penetration of dibucaine into palmitoyl-oleoyl phosphatidylcholine monolayers.[43] The high values obtained in the latter case might be due to the more expanded character of this partly unsaturated phospholipid membrane.

Atomic force microscopy, AFM, investigation

Further, AFM imaging yields important results on the structure and dynamics of lipid membranes at nanometer scale. Furthermore, AFM allows high resolution imaging of surfaces of membrane supramolecular assemblies leading to substantial new insights about the structure of lipid membranes in interaction with anesthetics.

For instance, AFM images revealed quantitative (measurable) details (Fig. 5) on various-sized LC domains (e.g., mainly nano-level domains) and their shapes (spherical, oval, squares, windmill aspect) occurred at a surface pressure of about 8 mN/m, during the phase transition of pure DPPC membrane where the LC and LE phases coexist.

These LC structures (Fig. 5) are compacted close together under the compression of the lipid membrane leading to the formation of rather large and flat vesicles within the DPPC monolayer (Fig. 6). The vesicles were detected at a surface pressure of 35 mN/m. The smooth DPPC membrane is characterized by low surface roughness, *i.e.*, RMS and Ra values of the height distribution, which are given in the legend of Figs. 5 and 6.

Further, the phase transformation from LE to LC is well evidenced on compressional isotherm given in Fig. 1A, on curve 1, at the surface pressure of about 35 mN/m, which is equivalent to the surface pressure indicated in Fig. 6. Thus, an interesting observation appears, namely the surface pressure is controlling the LC domain formation in DPPC membrane, as showed in Figs. 5 and 6.

In Fig. 6, a portion of a circular DPPC vesicle from condensed domain of about 6 μm in diameter is revealed at this surface pressure, which is much higher than the surface pressure given in Fig. 5. Finally, flat DPPC condensed domains are compressed near the collapse pressure of pure DPPC monolayer membrane (see, Fig. 1A, curve 1 and Table 1). Near the DPPC membrane collapse, vesicles are almost jointly condensed together leading to a DPPC smooth compact layer of very high stability.

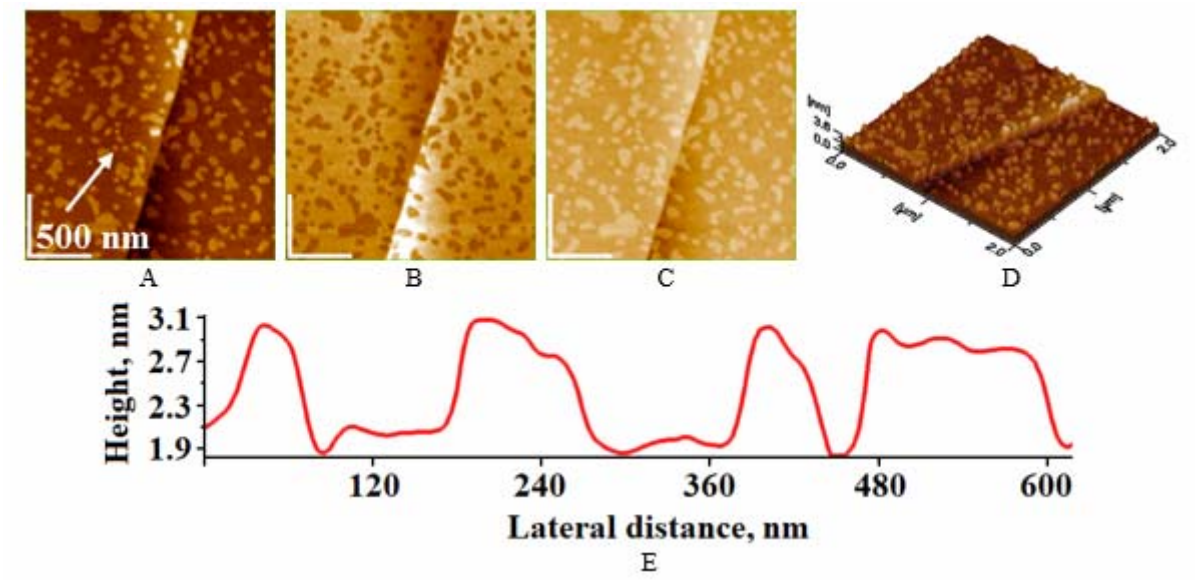

Fig. 5 – AFM images on pure DPPC monolayer membrane transferred on mica surface, at the onset of the LE to LC phase transition, at about 8 mN/m; A) 2D topographic image; B) phase image; C) amplitude image; D) 3D image; E) cross profile along the arrow in image (A); scanned area of 2 µm x 2 µm; RMS (root mean square) on scanned area 0.4 nm; RMS on cross profile 0.4 nm; Ra (arithmetic surface roughness) on scanned area 0.3 nm; Ra on profile 0.4 nm.

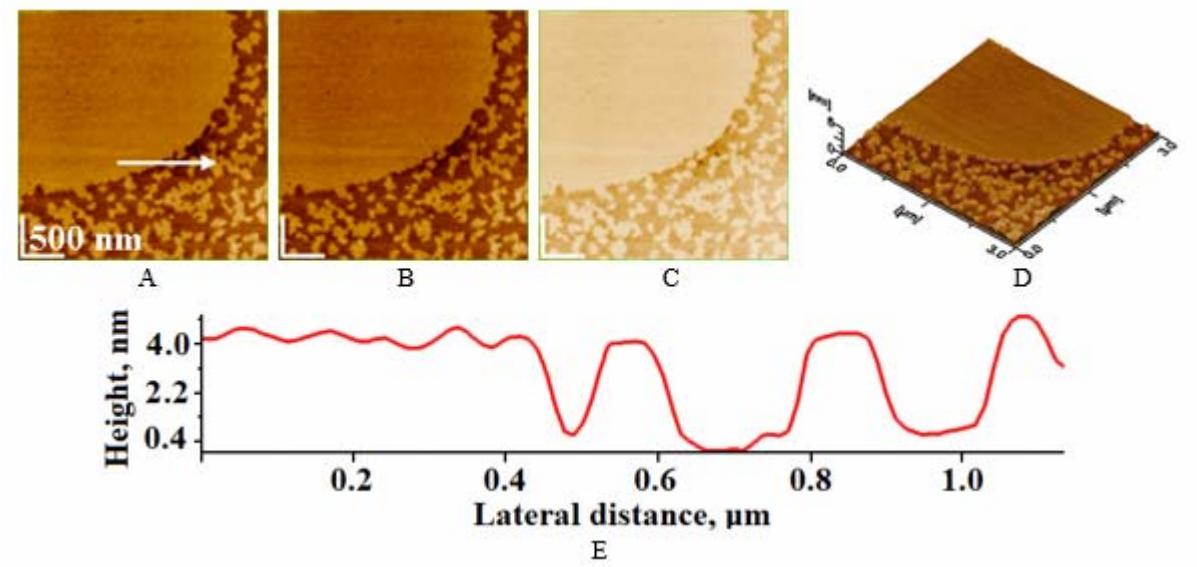

Fig. 6 – AFM images for pure DPPC monolayer membrane, transferred on mica surface at high surface pressure of about 35 mN/m; A-E images: symbols as in Fig. 5; scanned area of 3 µm x 3 µm; RMS on scanned area 0.3 nm; RMS on profile 0.4 nm; Ra on scanned area 0.2 nm; Ra on profile 0.3 nm.

The thickness of DPPC LC domain is predominantly around 31 Å (Fig. 5E) and the domain boundaries (Figs. 5A-D) were clearly observed in pure DPPC membrane at the phase transition LE/LC at 8 mN/m. In LC structures, the molecular packing of DPPC molecules, which are formed from hydrocarbon tails and head polar groups (i.e., ester along with zwitterion groups), is in substantial agreement with the molecular models proposed earlier for DPPC molecules[31] well packed at the air/water interface. Clearly, DPPC molecules are preferentially oriented with head groups predominantly parallel oriented to the air/water interface.[31] At higher surface pressures, like 35 mN/m, the membrane thickness of LC domains is about 40 Å (Fig. 6E), much higher than about 31 Å (Fig. 5E), indicating that the DPPC molecules are mainly packed with head groups predominantly perpendicular oriented to the air/water interface.[31]

The analogous situations are presented for DPPC monomolecular membrane on PR concentra-

tion of 10^{-4} M (Fig. 7) and 10^{-3} M (Figs. 8 and 9) in aqueous subphase at the surface pressure of about 8 mN/m for comparison with pure DPPC membrane structure given in Fig. 5. Very interestingly the thickness of LC domains of DPPC-PR membranes is almost the same of about 18 to 21 Å (Figs. 7E-9E), and much smaller than about 31 Å characteristic for LC of pure DPPC membrane (Fig. 5E). This situation indicates that the PR can modulate the fluidity of DPPC membrane by its penetration among the hydrocarbon tails of DPPC membrane and between the LC and LE domains at the phase transition from LE to LC mixed systems. This finding can be also interpreted that the molecular packing of DPPC molecules is perturbed by the adsorption of PR molecules on polar groups of DPPC molecules and also due to their penetration among the tails of hydrocarbons of DPPC membrane.

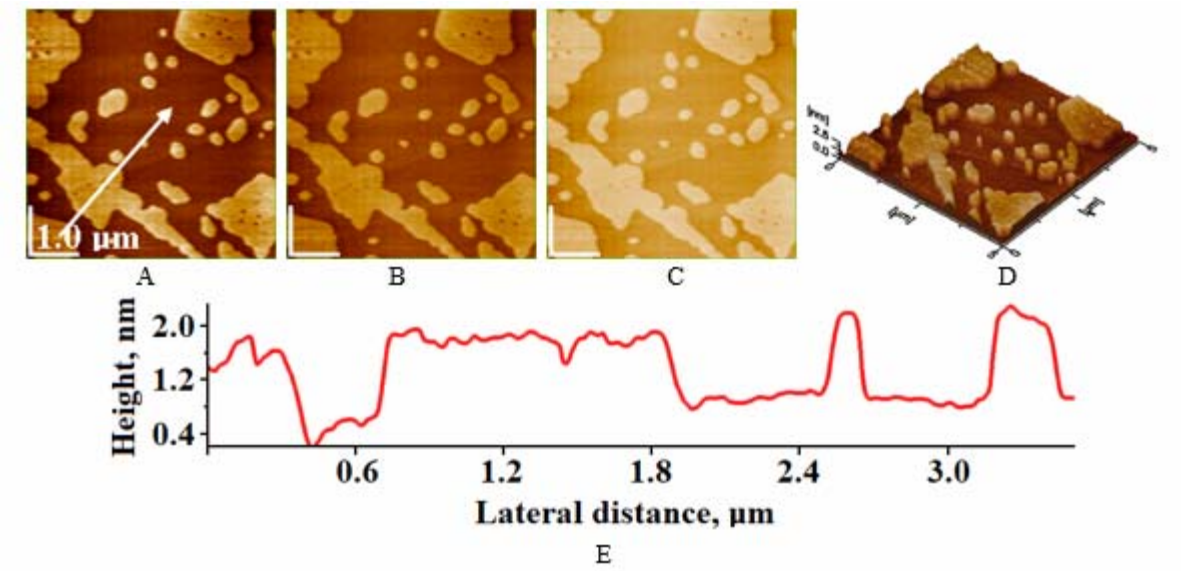

Fig. 7 – AFM images for DPPC monolayer membrane on PR (0.0001 M) substrate, transferred on mica surface, at the onset of LE/LC phase transition, at about 8 mN/m; A-E images: symbols as in Fig. 5; scanned area of 5 µm x 5 µm; RMS on scanned area 0.5 nm; RMS on cross profile 0.5 nm; Ra on scanned area 0.3 nm; Ra on profile 0.5 nm.

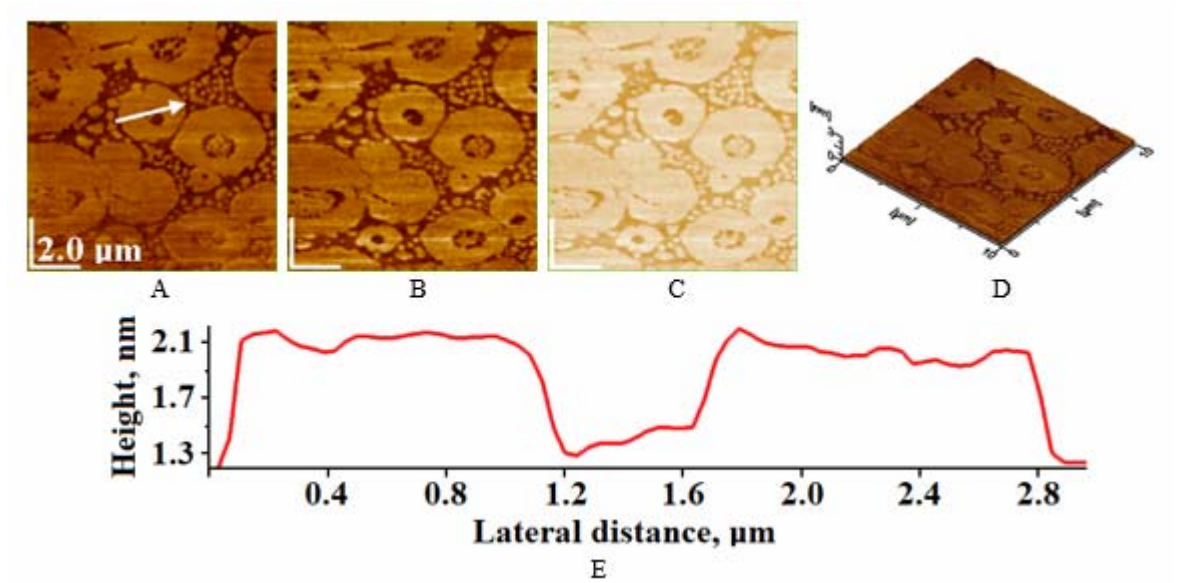

Fig. 8 – AFM images for DPPC monolayer membrane on PR (0.001 M) substrate, transferred on mica surface at surface pressure of about 8 mN/m; A-E images: symbols as in Fig. 5; scanned area of 10 µm x 10 µm; RMS on scanned area 0.3 nm; RMS on profile 0.3 nm; Ra on scanned area 0.2 nm; Ra on cross profile 0.3 nm.

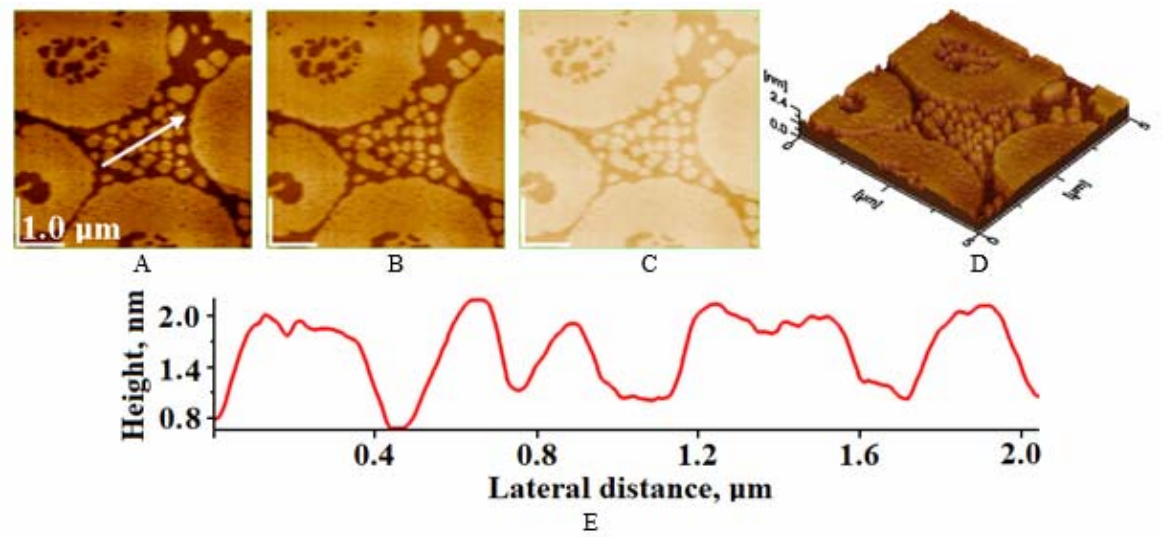

Fig. 9 – AFM images for DPPC monolayer membrane on PR (0.001 M) substrate, at the LE/LC phase transition, at about 8 mN/m; A-E images: symbols as in Fig. 5; scanned area of 5 µm x 5 µm; RMS on scanned area 0.3 nm; RMS on profile 0.3 nm; Ra on scanned area 0.2 nm; Ra profile 0.2 nm.

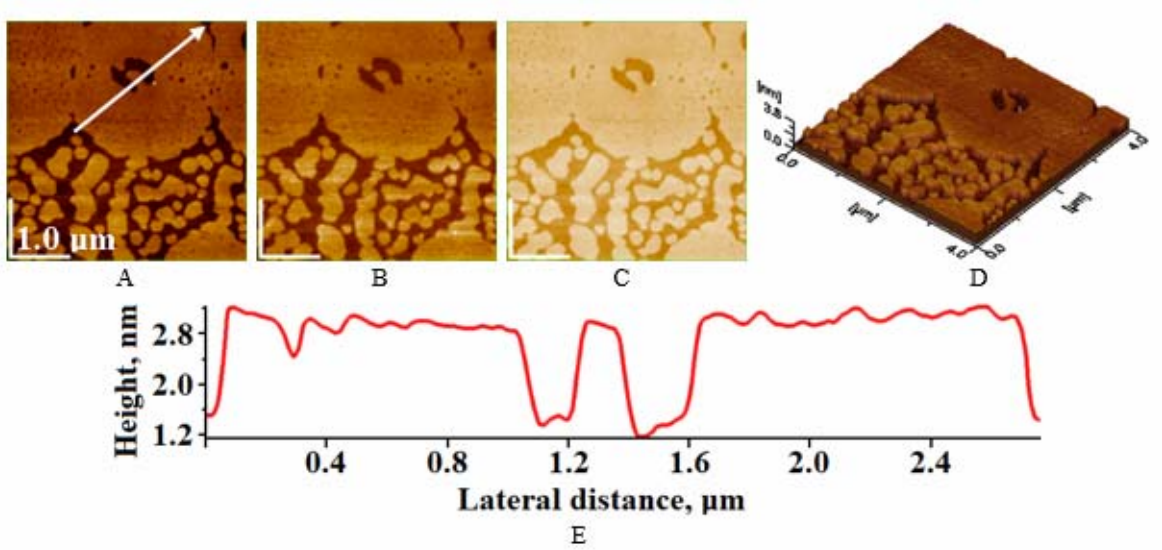

Fig. 10 – AFM images for DPPC monolayer membrane on PR (0.001 M) substrate, at about 35 mN/m; A-E images: symbols as in Fig. 5; sanned area of 4 µm x 4 µm; RMS on area 0.3 nm; RMS on profile 0.6 nm; Ra on area 0.2 nm; Ra on profile 0.5 nm.

In the presence of PR 10^{-4} M, in Fig 7, the shaped LC phospholipid domains were almost circular, oval or squares of various–sizes (*e.g.*, about 1 µm to 4 µm in diameter) in DPPC-PR membrane at the phase transition. At higher PR concentration, like 10^{-3} M in Figs 8 and 9, the DPPC-PR LC domains were almost circular vesicles of about 4 µm to 6 µm diameters at the phase transition, in the presence of many small LC domains existing in LE phase. The center of vesicles of about 1 µm was rather porous and occupied by LC small circular nano domains, (Figs. 8 and 9). The common boundary region of these vesicles appeared to define the condensation process of large vesicles with small DPPC-PR patches, or with smaller vesicles, through the phospholipid membrane compression, as seen in Figs. 8 A-D and 9 A-D.

Circular mixed vesicles of DPPC-PR, with condensed domains about 3 µm in diameter, were also revealed, in Fig. 10 A-D, fused together in DPPC membrane on PR (0.001 M) in aqueous phase at the surface pressure of about 35 mN/m. The DPPC-PR condensed domains are smaller than those observed in pure DPPC membrane (Fig. 6). The DPPC-PR, LC domains are further compressed close together near the collapse pressure of DPPC monolayer membrane on a 0.001 M procaine subphase (see Fig. 1, curve 3 and Table 1).

Increasing the surface pressure and thus, continuously decreasing the DPPC-PR membrane area, these vesicles were fused together and gave the network of almost circular vesicles, well oriented and jointly packed at the air/water interface and perfectly transferred on mica surface, by LB technology, as visualized in AFM images (Fig. 10A-D). In addition, the planar domains formed were reasonably circular. Therefore, we consider that their fusion is an approximately symmetric process.

The symmetric process is consistent with the fusion of large vesicles with small patches or small vesicles followed by an approximately equal spreading around the entire initial area of large vesicles. This mechanism of fusion process itself was directly observed due to high resolution AFM measurements.

The thickness of LC domains in mixed DPPC-PR membrane is around 33 Å (Fig. 10E) at 35 mN/m, much higher than 21 Å, which was found characteristic for LC domains of mixed DPPC-PR membrane at the phase transition at 8 mN/m (Figs. 8E and 9E). Consequently, the structural changes were discovered within DPPC membrane during the interaction with the local anesthetic procaine, which is an amphiphilic drug, by using AFM images and cross profiles.

Coupling thermodynamic approach with AFM investigation we analysed the procaine location and preferential orientation in DPPC membrane as well as the specific interactions of PR and DPPC model membrane. The charged polar group of procaine prefers the head group region of DPPC membrane, while uncharged amino group and benzene ring can penetrate in the hydrocarbon (tail) region of the phospholipid monolayer membrane. Procaine can also establish hydrogen bonds with phosphate and carbonyl moieties of the phospholipid in substantial agreement with molecular models used to investigate the behavior of procaine in lipid model membranes.

Our results led to a better understanding of the interaction between DPPC molecules within the Langmuir monolayer membrane and between the phospholipid membrane and procaine at a molecular level, in substantial agreement with vibrational spectroscopic approach[74,75] and molecular dynamic simulations.[76-78]

The effects of PRH^+ on the surface properties of DPPC monolayer membrane give further support for various hypotheses referenced as to how the phospholipids might be involved in anesthetic action. However, more work is needed before a detailed molecular mechanism involving phospholipids can be made to conform to physiological data on the behavior of various excitable membranes.

EXPERIMENTAL

Materials

L-α-dipalmitoyl phosphatidylcholine (DPPC) was purchased from Avanti Polar Lipids (Alabaster, AL). Procaine hydrochloride was obtained from Merck (Darmstadt, Germany). All chemicals were of analytical grade and were used without further purification. Procaine was dissolved in twice-distilled water.

Langmuir monolayer and compressional isotherms

The characteristic properties of biomolecules are firstly characterized by compressional isotherms which are crucial in obtaining a proper knowledge of what is occurring in model membranes at the molecular level. Secondly, AFM is used to obtain various images of LB transferred monolayer membrane on mica showing the membrane structure.

A comparison of the literature data shows that the surface pressure, π, *vs* mean molecular area, A, curves of DPPC monolayers are sensitive to the type of spreading solvent used.[24-30] Preliminary tests indicate that mixture (2:98, v/v) of absolute ethanol: n-hexane is sufficiently polar to dissolve the DPPC,[31] since the presence of ethanol affects both the surface tension and the physical state of the monolayer.[32] We attempted to minimize the effect of ethanol by spreading DPPC at relatively high ($\approx 10^{-3}$ M) phospholipid concentrations. Doubly-distilled water (pH ≈ 5.6) was used as an aqueous subphase. The reproducibility of the isotherms obtained from DPPC monolayers was checked following spreading by maintaining the film at high areas (A > 100$Å^2$ / molecule) for different time intervals (between 5 and 30 min) prior to compression. The π-A isotherms obtained were found to be practically identical irrespective of the waiting times, indicating that the DPPC monolayer isotherms were independent of the precompressional delay and the spreading solvent.

The surface pressure *versus* area curves were recorded continuously using the Wilhelmy method, as shown in Figs. 1A and 1B. Measurements revealed the shape of the isotherm to depend on the compressional speed at or above the LE/LC phase transition. Such effects have also been reported by other authors.[20,28,29] In our experiments, a compressional speed of 4-8 $Å^2$ $molecule^{-1}$ min^{-1} was used. This allowed a complete isotherm to be recorded in about 20-30 min with minimum data variation. The concentration range of used PR aqueous solutions was 0.001 mM-10 mM. The pH of the subphase was controlled between 5.1 and 5.6. At these values only the monocationic form (PRH^+) of procaine exists in aqueous solutions. All measurements were made at 22^0C. The accuracy of the surface pressure measurements was ± 0.25 mN/m while the π-A isotherm was selected from at least ten separate determinations, all made under identical conditions. DPPC monolayers were spread at the air/aqueous solution interface in the presence of procaine hydrochloride aqueous substrates and left about 15-30 min to attain equilibrium. At the air/water interface a mixed monolayer is formed that contains, besides water molecules (component 1), molecules of both surfactants,

protonated procaine (component 2), and phospholipid (component 3). All three components must be considered in order to understand the nature of drug-membrane interactions.

Langmuir-Blodgett, LB, transferred monolayers

Lipid monolayers were transferred by Langmuir-Blodgett technique, LBT, at different constant surface pressures,[44-53] on freshly cleaved muscovite mica surface, that were previously submerged in the aqueous subphase, as elsewhere described. The mica plate was fixed to a lifting device and was raised in the vertical plane out of the aqueous subphase at a constant speed of 8 $Å^2$/molecule, for every chosen constant surface pressure. Before the transfer, the lipid monolayer was equilibrated for 10 min at the selected constant surface pressure. The transfer ratio was equal to 1, namely without compression or expansion of the spread lipid monolayer either in the absence or in the presence of different concentrations in procaine. The LB film transfer took place at a speed of about 5 mm/min, which was tested as appropriate at each used constant surface pressure. Certainly, LBT improved the immobilization of monolayer membranes on mica substrate and made them accessible to high resolution imaging with AFM.

AFM measurements

Atomic force microscopy is a surface imaging technique with a nanometer-scale resolution.[54-64] AFM studies were performed using the AFM JEOL. The cantilevers were made of Si_3N_4, with a resonance frequency of 250 – 350 kHz. Through this study, AFM images were obtained at several constant surface pressures, like around 8 mN/m and 35 mN/m, in order to examine the effect of procaine on the phase transition from expanded liquid (LE) to condensed liquid (LC) in pure DPPC monolayers. In each situation, five to ten independent experiments were carried out, and up to 10 AFM images were taken and analyzed. The phospholipid membrane surface was also evaluated by surface roughness measurements[79,80] as shown elsewhere.

CONCLUSIONS

In this work, we studied the effects of procaine on a DPPC monolayer membrane. For the first time, the penetration of procaine into DPPC monolayers is explored by thermodynamic approach along with AFM investigation.

By recording surface pressure versus mean molecular area isotherms, the penetration of PRH^+ into DPPC monolayers was studied. Penetration number values derived for different π values allowed us to postulate the molecular mechanism of drug penetration. By collecting sequences of AFM images over a large monolayer membrane area, at various surface pressures, the conversion of isolated small patches and circular vesicles to large planar monolayer vesicles was observed.

One major conclusion is that the procaine concentration exerts a modulating influence on phospholipid (vesicles) LC domain structure and size along with the increasing of lateral surface pressures. Finally, the outcomes suggest that the pressure dependence of the procaine penetration into phospholipid model membranes might be of relevance in the interfacial mechanism of pressure reversal in anesthesia.

Acknowledgments: This research was funded by grants of the Ministry of Research, Innovation and Digitization, CNCS/CCCDI-UEFISCDI, project number 186 and 481, within PNCDI III.

REFERENCES

1. J. F. Butterworth and G. R. Strichartz, *Anesthesiology,* **1990**, *72*, 711-734.
2. I. Ueda, M. Hirakawa, K. Arakawa and H. Kamaya, *Anesthesiology,* **1986**, *64,* 67-71.
3. J. Shah, E. G. Votta-Velis and A. Borgeat, *Best Pract. Res. Clin. Anesthesiol.,* **2018**, *32,* 179-185.
4. P. T. Frangopol and D. Mihailescu, *Colloids Surf. B,* **2001**, *22,* 3-22.
5. D. A. Cadenhead, *Colloids Surf. B,* **2001**, *22,* 63-68.
6. M. Tomoaia-Cotisel, L. C. Stewart, M. Kates, J. Zsako, E. Chifu, A. Mocanu, P. T. Frangopol, L. J. Noe and P. J. Quinn, *Chem. Phys. Lipids,* **1999**, *100,* 41-54.
7. M. Tomoaia-Cotisel, *Progr. Colloid. Polym. Sci.,* **1990**, *83,* 155-166.
8. J. Zsako, M. Tomoaia-Cotisel, E. Chifu, I. Albu, A. Mocanu and P. T. Frangopol, *Rev. Roum. Chim.,* **1990**, *35,* 867-877.
9. J. Zsako, M. Tomoaia-Cotisel, I. Albu, A. Mocanu, E. Chifu and P. T. Frangopol, *Rev. Roum. Biochim.,* **1991**, *28,* 33-40.
10. M. Tomoaia-Cotisel, E. Chifu, A. Mocanu, J. Zsako, M. Salajan and P. T. Frangopol, *Rev. Roum. Biochim., **1988,** 25,* 227-237.
11. E. Chifu, M. Tomoaia-Cotisel, J. Zsako, A. Mocanu, M. Salajan, M. Neag and P. T. Frangopol, "Procaine penetration into uncharged stearic acid monolayers in terms of Gibbs' adsorption equation", in "Seminars in Biophysics", Vol. 6, P. T. Frangopol and V. V. Morariu (Eds.), IAP Press, Bucharest, 1990, p. 117-128.
12. M. Tomoaia-Cotisel, J. Zsako, A. Mocanu, E. Chifu, M. Salajan and S. Bran, *J. Colloid and Surface Chem.,* **1999**, *3,* 32-40.
13. E. Chifu, M. Tomoaia-Cotisel, J. Zsako, I. Albu, A. Mocanu and P. T. Frangopol, *Rev. Roum. Chim.,* **1990**, *35,* 879-889.
14. M. Tomoaia-Cotisel, T. Oproiu, J. Zsako, A. Mocanu, P. T. Frangopol and P. J. Quinn, *Rev. Roum. Chim*., **2000**, *45,* 851-861.
15. A.-N. Bondar, S. Shuhai, J. C. Smith and P. T. Frangopol, *Rom. Rep. Phys.,* **2007**, *59,* 289-299.
16. M. Tomoaia-Cotisel, J. Zsako, E. Chifu, P. T. Frangopol, W. A. P. Luck and E. Osawa, *Rev. Roum. Biochim.,* **1989**, *26,* 305-313.
17. M. Tomoaia-Cotisel and D. A. Cadenhead, *Langmuir,* **1991**, *7,* 964-974.
18. B. Asgharian, D. A. Cadenhead and M. Tomoaia-Cotisel, *Langmuir,* **1993**, *9,* 228-232.

19. D. Chapman, *Quarterly Reviews in Biophysics,* **1975**, *8,* 185-235.
20. D. A. Cadenhead, "Monomolecular films as biomembrane models", in "Structure and properties of cell membranes", Vol. 3, Gh. Benga (Ed.), CRC Press, Boca Raton, 1985, p. 21-62.
21. P. Tancrede, G. Munger and R. M. Leblanc, *Biochim Biophys. Acta,* **1982**, *689,* 45-54.
22. E. C. Kelusky and I. C. P. Smith, *Biochem.,* **1983**, *22,* 6011-6017.
23. E. C. Kelusky and I. C. P. Smith, *Can. J. Biochem. Cell Bio.,* **1984**, *62*, 178-184.
24. J. C. Watkins, *Biochim. Biophys. Acta,* **1968**, *152,* 293-306.
25. P. Joos and R. A. Demel, *Biochim. Biophys. Acta,* **1969**, *183,* 447-457.
26. J. W. Munden and J. Swarbrick, *J. Colloid Interface Sci.,* **1973**, *42,* 657-659.
27. D. A. Cadenhead and B. M. J. Kellner, *J. Colloid Interface Sci.,* **1974**, *49,* 143-145.
28. F. Vilallonga, *Biochim. Biophys. Acta,* **1968**, *163*, 290-300.
29. M. C. Phillips and D. Chapman, *Biochim. Biophys. Acta,* **1968**, *163,* 301-313.
30. M. Hayashi, T. Muramatsu and I. Hara, *Biochim. Biophys. Acta,* **1972**, *255,* 98-106.
31. M. Tomoaia-Cotisel, J. Zsako and E. Chifu, *Ann. Chim. (Rome),* **1981**, *71,* 189-200.
32. D. A. Cadenhead and J. E. Osonka, *J. Colloid Interface Sci.,* **1970**, *33,* 188-191.
33. B. A. Pethica, *Trans. Faraday Soc.,* **1955**, *51,* 1402-1411.
34. M. Nakagaki and E. Okamura, *Bull. Chem. Soc. Japan,* **1982**, *55,* 1352-1356.
35. M. Nakagaki and E. Okamura, *Bull. Chem. Soc. Japan,* **1982**, *55,* 3381-3385.
36. M. Nakagaki and E. Okamura, *Bull. Chem. Soc. Japan,* **1983**, *56,* 1607-1611.
37. G. Beurer and H.-G. Galla, *Eur. Biophys. J.,* **1987**, *14,* 403-408.
38. M. Tomoaia-Cotisel, J. Zsako, A. Mocanu, M. Salajan, Cs. Racz, S. Bran and E. Chifu, *Stud. Univ. Babes-Bolyai Chem.,* **2003**, *48,* 201-218.
39. J. Zsako, M. Tomoaia-Cotisel, E. Chifu, A. Mocanu and P. T. Frangopol, *Biochim. Biophys. Acta,* **1990**, *1024,* 227-232.
40. J. Zsako, M. Tomoaia-Cotisel, E. Chifu, A. Mocanu and P. T. Frangopol, *Gazz. Chim. Ital.*, **1994**, *124,* 5-9.
41. J. Zsako, E. Chifu, M. Tomoaia-Cotisel, A. Mocanu and P. T. Frangopol, *Rev. Roum. Chim.,* **1994**, *39,* 777-786.
42. J. M. Crane, G. Putz and S. B. Hall, *Biophys. J.,* **1999**, *77,* 3134-3143.
43. A. Seelig, *Cell Biol. Int. Rep.,* **1990**, *14,* 369-380.
44. M. Tomoaia-Cotisel and A. Mocanu, *Rev. Chim.,* **2008**, *59,* 1230-1233.
45. P. T. Frangopol, D. A. Cadenhead, M. Tomoaia-Cotisel and A. Mocanu, *Stud. Univ. Babeş-Bolyai Chem.,* **2009**, *54,* 23-35.
46. P.T. Frangopol. D. A. Cadenhead, Gh. Tomoaia, A. Mocanu, M. Tomoaia-Cotisel, *Rev. Roum. Chim.*, **2015**, *60*, 265-273.
47. M. Tomoaia-Cotisel, Gh. Tomoaia, A. Mocanu, V.-D. Pop, N. Apetroaei and Gh. Popa, *Stud. Univ. Babeş-Bolyai Chem.*, **2004**, *49,* 167-181.
48. Tomoaia-Cotisel, Gh. Tomoaia, V.-D. Pop, A. Mocanu, O. Cozar, N. Apetroaei and Gh. Popa, *Stud. Univ. Babeş-Bolyai Phys.*, **2004**, *49,* 141-152.
49. M. Tomoaia-Cotisel, Gh. Tomoaia, V.-D. Pop, A. Mocanu, N. Apetroaei and Gh. Popa, *Rev. Roum. Chim.,* **2005**, *50,* 381-390.
50. M. Tomoaia-Cotisel, Gh. Tomoaia, V.-D. Pop, A. Mocanu, O. Cozar, N. Apetroaei and Gh. Popa, *Rev. Roum. Chim.,* **2005**, *50,* 471-478.
51. M. Tomoaia-Cotisel, V. D. Pop, Gh. Tomoaia, A. Mocanu, Cs. Racz, C. R. Ispas, O. Pascu and O. C. Borostean, *Stud. Univ. Babeş-Bolyai Chem.*, **2005**, *50,* 23-37.
52. M. Tomoaia-Cotisel, A. Tomoaia-Cotisel, T. Yupsanis, Gh. Tomoaia, I. Balea, A Mocanu and Cs. Racz, *Rev. Roum. Chim.,* **2006**, *51,* 1181-1185.
53. I. Cojocaru, A. Tomoaia-Cotisel, A. Mocanu, T. Yupsanis and M. Tomoaia-Cotisel, *Rev. Chim.,* **2017**, *68,* 1470-1475.
54. A. Stylianou, *J. Nanomater.*, **2017**, *2017,* 9234627-9234641
55. E. I. Goks, J. M. Vanegas, C. D. Blanchette, W.-C. Lin and M. L. Longo, *Biochim. Biophys. Acta,* **2009,** *1788,* 254-266.
56. K. El Kirat, S. Morandat and Y. F. Dufrene, *Biochim. Biophys. Acta,* **2010**, *1798,* 750-765.
57. A. Hidalgo, C. Garcia-Mouton, C. Autilio, P. Carravilla, G. Orellana, M. N. Islam, J. Bhattacharya, S. Bhattacharya, A. Cruz and J. Pérez-Gil, *J. Control. Release*, **2021**, *329*, 205–222.
58. L. Xu, Y. Yang and Y. Y. Zuo, *Biophys. J.*, **2020**, *119*, 756-766.
59. O. G. Andriotis, W. Manuyakorn, J. Zekonyte, O. L. Katsamenis, S. Fabri, P. H. Howarth, D. E. Davies, P. J. Thurner, *J. Mech. Behav. Biomed. Mater*., **2014**, *39*, 9-26.
60. Y. F. Dufrene and G. U. Lee, *Biochim. Biophys. Acta,* **2000***, 1509*, 14-41.
61. C. Hao, R. Sun and J. Zhang, *Colloids Surf. B,* **2013**, *112,* 441-445.
62. M. Deleu, K. Nott, R. Brasseur, P. Jacques, P. Thonart and Y. F. Dufrene, *Biochim. Biophys. Acta,* **2001**, *1513*, 55-62.
63. Gh. Tomoaia, P. T. Frangopol, O. Horovitz, L.-D. Bobos, A. Mocanu and M. Tomoaia-Cotisel, *J. Nanosci. Nanotechnol.,* **2011**, *11,* 7762-7770.
64. A. Mocanu, R. D. Pasca, Gh. Tomoaia, C. Garbo, P. T. Frangopol, O. Horovitz and M. Tomoaia-Cotisel, *Int. J. Nanomed.,* **2013**, *8,* 3867-3874.
65. P. T. Frangopol, A. Mocanu, V. Almasan, C. Garbo, R. Balint, G. Borodi, I. Bratu, O. Horovitz and M. Tomoaia-Cotisel, *Rev. Roum. Chim.,* **2016**, *61,* 337-344.
66. O. Cadar, P. T. Frangopol, Gh. Tomoaia, D. Oltean, G. A. Paltinean, A. Mocanu, O. Horovitz and M. Tomoaia-Cotisel, *Stud. Univ. Babeş-Bolyai Chem.,* **2017**, *62,* 67-80.
67. S. Rapuntean, P. T. Frangopol, I. Hodisan, Gh. Tomoaia, D. Oltean-Dan, A. Mocanu, C. Prejmerean, O. Soritau, L. Z. Racz, and M. Tomoaia-Cotisel, *Rev. Chim.* (*Bucharest*)*,* **2018**, *69,* 3537-3444.
68. D. Oltean-Dan, P.T. Frangopol, R. Balint, Gh. Tomoaia, A. Mocanu and M. Tomoaia-Cotisel, *Stud. Univ. Babeş-Bolyai Chem.*, **2021**, *66,* 73-87.
69. R. Balint, I. Petean, P. T. Frangopol, A. Mocanu, G. Arghir, S. Riga, Gh. Tomoaia, O. Horovitz and M**.** Tomoaia-Cotisel, *Stud. Univ. Babeş-Bolyai Chem.*, **2021**, *66*, 141-160.
70. A. Mocanu, P.T. Frangopol, R. Balint, O. Cadar, I.M. Vancea, R. Mintau, O. Horovitz and M. Tomoaia-Cotisel, *Stud. Univ. Babeş-Bolyai Chem.*, **2021**, *66*, 195-207.
71. A. Mocanu, O. Cadar, P. T. Frangopol, I. Petean, Gh. Tomoaia, G.-A. Paltinean, C. P. Racz, O. Horovitz and

M. Tomoaia-Cotisel, *R. Soc. Open. Sci.*, **2021**, *8*, 201785-201816.
72. O. Horovitz, Gh. Tomoaia, A. Mocanu, T. Yupsanis and M. Tomoaia-Cotisel, *Gold Bull.,* **2007**, *40,* 295-304.
73. Gh. Tomoaia, M. Tomoaia-Cotisel, A. Mocanu, O. Horovitz, L.D. Bobos, M. Crisan and I. Petean, *J. Optoelectron. Adv. Mater.,* **2008**, *10,* 961-964.
74. M. Tomoaia-Cotisel, E. Chifu, S. Jitian, I. Bratu, S. Bran, P. T. Frangopol and A. Mocanu, *Stud. Univ. Babeş-Bolyai, Chem.*, **1990**, *35*, 17-24.
75. Y. Sheeba Sherlin, T. Vijaykumar, J. Binoy, S. D. D. Roy and V. S. Jayakumar, *Spectrochim. Acta A Mol. Biomol. Spectrosc.,* **2018**, *205,* 55-65.
76. P. A. Zapata-Morin, F. J. Sierra-Valdez and J. C. Ruiz-Suarez, *J. Mol. Graph. Model.,* **2014**, *53,* 200-205.
77. S. Jalili and M. Saeedi, *Eur. Biophys. J.,* **2017**, *46,* 265-282.
78. M. S. Ali, M. A. Farah, H. A. Al-Lohedan and K. M. Al-Anazi, *RCS Adv.,* **2018**, *8,* 9083-9093.
79. U. V. Zdrenghea, Gh. Tomoaia, D. V. Pop-Toader, A. Mocanu, O. Horovitz and M. Tomoaia-Cotisel, *Comb. Chem. High Throughput Screen,* **2011,** *14,* 237-247.
80. D. Oltean-Dan, G. B. Dogaru,–E. M. Jianu, S. Riga, M. Tomoaia-Cotisel, A. Mocanu, L. Barbu-Tudoran and Gh. Tomoaia, *Micromachines,* **2021**, *12,* 1352-1376.